Design Optimization of a Rotor for Flywheel Energy Storage System

Kainat Riaz[1], Syeda Fatima Imam[1], Nida Ilyas[1], Zia ul Rehman Tahir[1,*], Muhammad Taimoor Adil[1], Sajeer Ahmad[1], Muhammad Abdullah[1], Tariq Ali[1], Imran Amin[1], Ahmad Hassan[1], Najum ud Din[1], Muhammad Saad[1]

[1] *Department of Mechanical Engineering, University of Engineering and Technology Lahore, Pakistan*
[*] *Corresponding author. Email: ziartahir@uet.edu.pk*

ABSTRACT
Flywheel Energy Storage System (FESS) is an emerging technology with notable applications. To conduct analysis of flywheel's rotors, cylindrical shape optimization considering steel material is an untapped research domain. This is the first-ever shape optimization study in which the main focus is to design and optimize shape of flywheel's rotor with different combinations of radius and thickness by keeping constant rotational speed (50,000 rpm with one-hour retention time), energy storage capacity (50 kW) and material properties (steel). A shape optimization analysis was performed for four different shapes (cylindrical, laval, conical and oval) to find the most suitable for rotor design. The suitable combinations of rotor thickness and radius of the selected shape were determined for maximum energy storage value (180-190 MJ) within commercially available ranges (10-2080 mm and 30-600 mm). A static analysis was conducted to calculate stresses and deformations for these combinations and best ones were selected based on lowest values. The narrowed down limits of these values were used for second optimization to increase precision. The intersecting combinations of radius and thickness (when compared with stress and displacement) were used as input in third optimization. Four different cases were performed on the finest combination to introduce non-homogeneities in the homogenous model. The final model was obtained by converging dimensions from each case experiencing the least stress and displacement. The diameter (hub diameter) and outer (inner) thickness of converged model were 377.1 mm (90 mm) and 1022.7 mm (755.9 mm) respectively, the model was curved inward at 882.6 mm. The minimum stress and displacement observed for this model were 11.8 GPa and 5.09 mm respectively. The study uses general static analysis in which aerodynamics, friction and vibrations were ignored. To improve results, an approach of using dynamic analysis (rotor balancing and aerodynamic system) and composite materials can be considered.

Keywords: *Flywheel energy storage systems, Shape optimization, Flywheel rotor design, Optimum radius to thickness ratio.*

1. INTRODUCTION

A Flywheel Energy Storage System (FESS) is a big mechanical battery that operates by storing electrical energy from a motor in the form of kinetic energy [1]. FESS uses the rotating mass principle to store energy and stores rotational kinetic energy. When FESS is charging it speeds up to store the provided energy and when it slows down it discharges to deliver the stored energy. An electrical motor/generator is used to drive the flywheel and convert electrical energy to mechanical energy and vice versa [2, 3]. The controlling motor/generator controls the flywheel because they are coaxially connected. The aim of this paper is to design and optimize the rotor of FESS which can deliver power of 50 kW at 50000 rpm with retention time of 1 hour.

Renewable energy storage devices are instantaneous power, reduced carbon emissions, longer lifetime, larger efficiency, and high charging and discharging rates which are similar characteristics of FESS to make it suitable and unique [4]. The rotational speed of the flywheel can be used easily to determine the state of charge and that state of charge is not affected by temperature or life. Some disadvantages are that the flywheel can be hazardous as it rotates at high rotational speed and in case of any failure of the flywheel breakdowns, the small piece flies around and can be fatal.

One of the most favourable features of FESS is its low operational maintenance [5]. Flywheels do not need long cycles and can perform for longer periods without much deterioration in their condition as compared to other energy devices. FESS can provide an efficiency of 90-

95 % with a high-power density [6]. Charging and discharging of FESS is efficient and quick based on the application and functionality. FESS is an environment-friendly system as no harmful substance is involved in its functioning and has no carbon footprint. The power and energy are independent of the system delivered by FESS. The energy provided by FESS is determined by the material, size of the rotor, and speed. The power rating of FESS is dictated by the electronics being used in the system for example, motor/generator [7, 8].

Rotor dynamics is used to study the vibration behaviour of rotating structures. A permanent failure is occurred as the result of larger amplitude vibrations which bend and twist the rotors [9]. These days high-speed turbomachines are key components of the rotating structure that is used in power stations, automobiles, and high-speed jet engines. This rotating structure is referred to as "Rotors" [10]. Resonance develops when these rotors rotate at a very high speed. These Rotors vibrate when harmonics loads are excited at their natural frequency in the state of resonance [11].

When comparing the electrochemical batteries and FESS, it is observed that specific power for FESS can vary anywhere from 5 kW/kg to 10 kW/kg and modern FESS can have specific power beyond 200 Wh/ kg [12]. Whereas specific power for lead-acid batteries can only be up to 30 Wh/kg. This situation, however, is reversed when FESS and electrochemical batteries are compared on the basis of their cost.[8]. Energy recovery efficiency must also be included in this cost analysis. Latest electrochemical batteries are efficient up to 60 to 70% whereas FESS can have 90 to 95 % efficiency. There are many other advantages of FESS including lower environmental impact as no substance is involved in its working and their ability to work over a wide range of temperatures [8].

The performance of FESS can be improved by using high operating speed, higher strength materials, or by shape and dimension optimization of its rotor [12]. Babuska et al. analysed the shape and rotational stress of FESS [13]. Based on rotor material flywheel has two main classes. First-class uses the new composite material like carbon fibers/graphite. These advanced materials have a higher strength-to-weight ratio, this provides the flywheel with higher specific energy. The second class of flywheel uses the main structural material in the rotor. This not only includes the traditional designs with larger diameters, slow rotation, and low energy densities and power but also includes some new higher-performance flywheels [14]. In the past iron and other classical materials are used for analysis but new fiber materials make the rotor lighter in weight with higher rotational speeds [15]. In this study, steel has been chosen as the rotor material as it is cheaper and much more easily available than fibre materials. In past research, no such analysis or optimization of steel rotors has been done.

The cylindrical rotor of FESS has mass of about 1.5 tonnes and has maximum angular velocity of about 314 rad/sec. During the normal operation, deceleration of rotor is about half of this maximum speed. Modern flywheels typically run at speed exceeding 10,000 rpm. This means that usually high-strength materials are suitable for systems like FESS. To minimize the energy losses due to friction vacuum enclosure and magnetic bearing system are frequently used [16]. The reduction of radial tensile stresses is in the middle part of the rotor design for a high-speed FESS design. Radial stresses of flywheel rotors can be reduced by a properly designed hub construction. A conforming hub structure to the specified conditions under the action of centrifugal forces is the solution to this. Ha, Kim et al [17] propose a hub structure that is separated at numerous points along its length. Required radial compressive load can be imposed on the inside surface of the rotor by the sections of the hub.

The rotor material and design selections are also important parameters to the design of the flywheel structure that connects the rotor to the electrical machine. There can be two types of assemblies for rotation of rotor; either the rotor is connected directly to the motor, or the motor drives a shaft which then turns the rotor. Stresses are generated during the motion of the rotor in the circumference direction as well as in the radial directions due to the acting centrifugal forces. The high strength materials are used when the hoop tensile stresses are dominant. The hoop stresses are not uniform in the radial direction. For single-material rotors, the maximum tensile hoop is mostly inside the rotor [16]. According to the analysis of more and more countries, a wide range of new laws and technological issues make the future of their energy sustainable [18].

According to the US Department of Defence, future combat vehicles can have electric propulsion as well as suspension, communications, weapons, and defensive systems, all require electricity. As a result, the flywheels can provide both continuous and pulsed power to the different subsystem controls and power-conditioning devices on the vehicle distribution networks [12]. During the 1960s and 1970s, a NASA-sponsored program proposes FESS as a possible primary source for a space mission. FESS is also used for vehicles and stationary power backup as a primary objective [19]. Fibre composite rotors are built and analysed in the US Flywheel Systems (USFS) lab and other organizations. The current model at USFS has been tested and the results show that the power densities at 110,000 rpm, its designed speed will exceed 11.9 kW/kg within 93 % efficiency [13].

The University of Texas at Austin has put a composite flywheel spinning at around 48,000 rpm through more than 90,000 charge-discharge cycles without losing function [8]. The institution is currently also developing a FESS which upon its operation can deliver 360 MJ of energy and 2 MW of power. The same university is also testing the function of FESS for accelerating a hybrid electric bus up to 100 km/h and storing 7.2 MJ of energy. The same system can provide more than 12 kJ/kg of specific energy and 2.5 kW/kg worth of power [21].

The use of an energy storage unit is more attractive and its results are expected. The flywheel proves an efficient ideal energy storage unit with a longer life cycle, more operating temperature range, free from depth-of-discharge effect, and higher power and energy density on both a mass and a volume basis [22]. In ancient times, devices employing the concept of kinetic energy storage were pottery wheels and spinning wheels in a rotating mass. With the advancement of technology and modern equipment, flywheels have become more common and conventional to use. Modern machinery like steam engines and Internal Combustion (IC) engines need systems like these to smooth out the inconsistent behaviour of torque triggered by the reciprocating movement of pistons [16]. Hu et al. [23] study aims to design a rotor dynamics model and analyse the flywheel rotor which has a 200 W storage capacity at 20,0000 rpm rotational speed and 4 Nm maximum input torque for the rotor. The results examined from this study show that maximum total deformation along the rotor shaft occurs at 0.00002154 mm, and maximum and minimum stresses are 0.681 MPa and 0.085153 MPa respectively. It observes that if rotor rotational speed exceeds its critical limits, its behaviour gyroscopically affects the model resulting in various degrees of deformation and mechanical failure.

Hodžić et al. [24] study aims to investigate the effect of working conditions on the mechanical behaviour of a rotor and perform the numerical analysis of the rotor of a high-speed integrated FESS. To investigate the centrifugal force of the rotor is subjected to a 75000 rpm angular velocity. Stress analysis results show that maximum stresses along the axis for circular disc and sinusoidal disc maximum stresses on the surface. Frequency analysis shows that resonance does not occur when natural frequency modes are above force frequency. Resonance occurs when the angular velocity is above 120,000 rpm. For electric utilities, short-duration energy storage is important to enhance the reliability and robustness of the grid. For short time durations, the flywheel has become a feasible means like frequency regulation, voltage levelling, and fault ride-through support of intermittent sources such as wind and solar farms [25].

Shape factor K mainly depends on the rotor geometry. Stress distributes in bi-directional rotor design with a shape factor > 0.5. These stresses cannot be handled by filament wound composite rotors with unidirectional laminates, since transverse tensile strengths are very low in the radial direction. An alternative manufacturing method must be used if rotor design with a shape factor ≤ 0.5, which results in a multi-directional composite, with better transverse tensile strength and lower hoop strength. Metal rotors can be fabricated for high shape factors. The selection of material rotor also depends on the shape factor [26, 27].

The present study has two objectives. First objective is to find the best thickness distribution of a flywheel rotor along the centrally bored radius. Second objective is to find whether the composite rotors are better than the metals or not. Four shapes were considered initially for the decision of material: Laval, cylindrical, oval and conical. Stresses were observed in these four shapes for three different materials: steel titanium alloy and fibre glass. Although fibre glass experienced least stresses, steel was chosen as the rotor material because of its availability and lower cost. Diameter and thickness of the rotor were determined through MATLAB, and it was modelled on SolidWorks. Simulations were run on the rotor on Abaqus according to the provided parameters and stress and displacement values were noted. The designed rotor was then optimized two times for diameter and thickness before concluding the final model for the rotor.

2. METHODOLOGY

In this study a rotor for Flywheel Energy Storage System is designed and optimized. The power requirement for the designed rotor is 50 kW at 50000 rpm with retention time of 1 hour. Computer aided designing and finite element analysis is used to design this rotor. In this section, the methodology for the design is presented. Geometry modelling, boundary conditions, load conditions, meshing of the flywheel rotor, and optimization is described in this section.

Commercial finite element analysis software Abaqus, was used to develop a procedure for optimizing structural shape. Abaqus is Computer Aided Engineering Software (CAE) used to model and analyze mechanical components and visualize their FEA results. The shaft and rotor were considered as a cylinder and a concentric ring. The shape optimization procedure was started with a "non-integrated design" flywheel, which means shaft and rotor are not integrated as a single unit. A rigid installation was used to connect the flywheel and its drive shaft, no key-ways were needed to fix/drive the flywheel, no built-in stress or deformations on the connection

surface, therefore displacement constraints can be simply applied on the shaft hole. The flywheel only worked in the vertical plane (X-Y plane) so that the gravity could be simply applied, and the fillets/chamfers could be neglected unless dimensioned.

Initially, shape optimization analysis was performed for four different shapes (cylindrical, Laval, conical and oval) to find the most suitable shape for rotor design. The objective was to enhance the energy density of the flywheel rotor by improving the geometry shape of the rotor, resulting in an equitable stress distribution. Flywheel with a consistent density of material and rotational speed was used and parameters of flywheel were taken as 50000 rpm, 50 kW power and, density and elastic modulus of flywheel material was 7850 kg/m^3 and 200 GPa respectively.

$$E = \frac{\pi}{4}\rho R^4 t\omega^2 \quad (1)$$

Equation (1) could be used to compute the maximum energy storage capacity of the flywheel. R is the radius, t is the thickness, ω is the angular velocity and ρ is the density of the flywheel. Constant power was required, the energy capacity required is

$$E = Pt \quad (2)$$

Using above Equation (2), the value of the maximum energy storage capacity of the flywheel was 180 MJ. MATLAB was used to develop a code using Equation (1) to find the combinations for R4t to determine the values for radius and thickness. The suitable combinations of rotor thickness and radius of the selected shape were determined for maximum energy storage value (180-190 MJ) within commercially available ranges (10-2080 mm and 30-600 mm respectively).

SolidWorks was used to model the flywheel rotor according to the dimensions mentioned in Table 1. According to the simplified model, an even-stress shape design does not exist for bore radii greater than the square root of one-third of the radius of the flywheel [27]. The optimum-shape predictions of models agree well if the radius of the bore does not exceed approximately one-third of the radius of the disk. Hub diameter was calculated as the square root of one-third of the external diameter. Four different cases were considered to make the rotor non-uniform and introduced non-homogeneity in a homogenous cylinder.as given in Table 3. One dimension (i.e., the second one in each case) was chosen from the third optimization based on least stresses and displacement. This dimension was then varied ±15% while keeping the other dimensions constant. Stress and displacement were observed for each case. The model showing the least stress and displacement in each case was converted into a single model to give the most optimum rotor shape.

2.1. Boundary and Load Conditions

Displacement/rotation boundary condition was applied to the internal hub of the flywheel. Displacement was zero along all axes and rotational displacement was zero along the X and Z axes as shown in Figure 1(b). Rotational displacement along Y-axis was allowed. A load of 5236 rad/sec was applied to the whole flywheel as rotational body force while keeping the uniform distributions as shown in Figure 1(a).

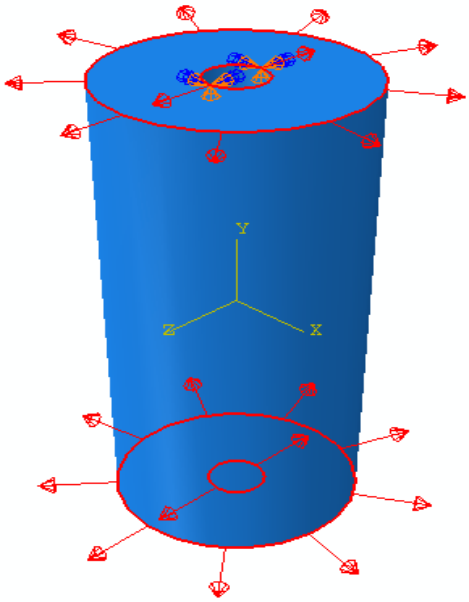

(a)

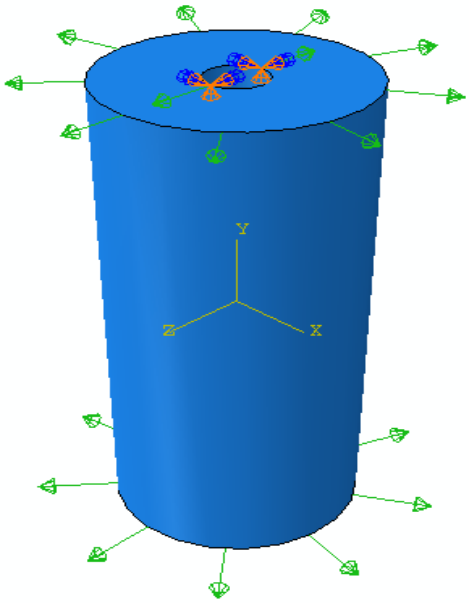

(b)

Figure 1 (a) Load conditions (b) Boundary conditions

2.2. Meshing

Free mesh with a seeding size of 65 mm was adopted to mesh the model. In terms of shape element, the free mesh has no restrictions. The whole flywheel meshed as tetrahedral elements as shown in Figure 2.

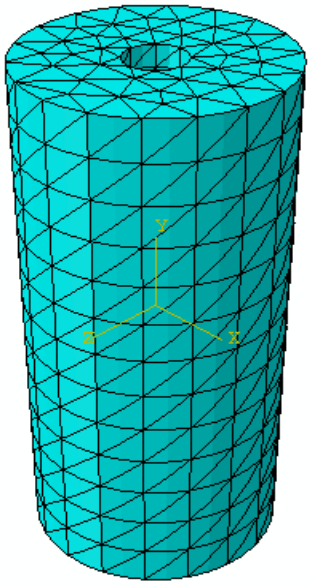

Figure 2 Meshing of finished model

3. RESULTS AND DISCUSSION

The objective of this analysis was to study the different diameter and thickness combinations for the flywheel and select the most appropriate combination for further analysis. Figure 3 shows Von Misses stresses against different shapes, the shapes were selected before optimization to find the most suitable shape for rotor design. The cylindrical shape is the most suitable one because it undergoes the least Von Misses stresses. Fiberglass is the most preferred material for rotor but steel was selected in this study because it is most commonly available in the market and cheaper than the other two materials (Titanium Alloy and Fiberglass).

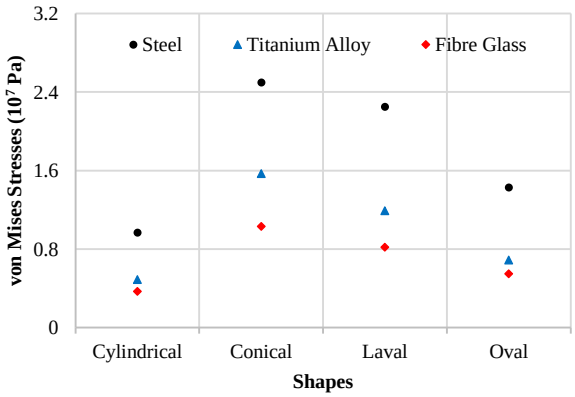

Figure 3 Comparison of different shapes of flywheel rotor

3.1. Optimization 1

Graph shown in Figure 4 was acquired from the code.

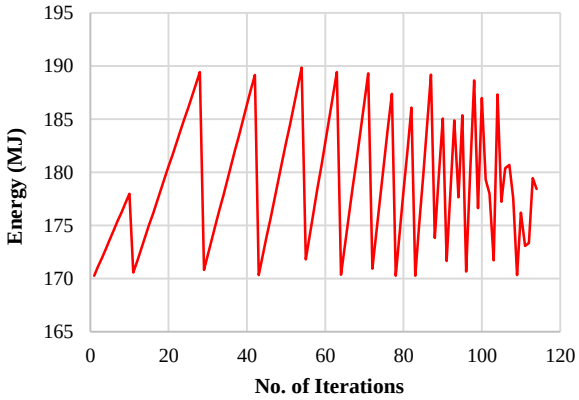

Figure 4 First Possible set of combinations of radius and thickness

These peak combinations of radius and thickness from this graph were used for modeling and analysis. Table 1 shows these values.

Table 1 Initial Thickness and Diameter Combinations

Configuration No.	Diameter (mm)	Thickness (mm)	Stresses (GPa)	Deflection (mm)
C1	320	1710	5.49	0.903
C2	340	1340	6.169	1.124
C3	360	1070	7.08	1.372
C4	380	860	7.84	1.623
C5	400	700	8.1	1.857
C6	420	570	8.98	2.049
C7	440	470	9.446	2.206
C8	460	400	10.05	2.358
C9	480	330	10.78	2.524
C10	500	280	12.02	2.808
C11	520	240	11.94	3.202
C12	540	210	12.15	3.634
C13	560	180	12.75	4.086
C14	620	120	13.73	5.589

The results from Abaqus were used to plot graphs for stresses and deflection for all of the radius and thickness combinations. Deflection and stresses were plotted separately against thickness and diameter as shown in Figure 5(a) and 5(b). Figure 5(a) shows with the increases in thickness the stresses in the flywheel decrease, the inverse relationship can be explained by the fact that as the thickness of a body increases the stiffness and resisting area for applied load also increases. On the other hand, as diameter increases the stresses also increase as shown in Figure 5(b), the reason is as the diameter increases the body is more prone to cracks and residual stresses [30].

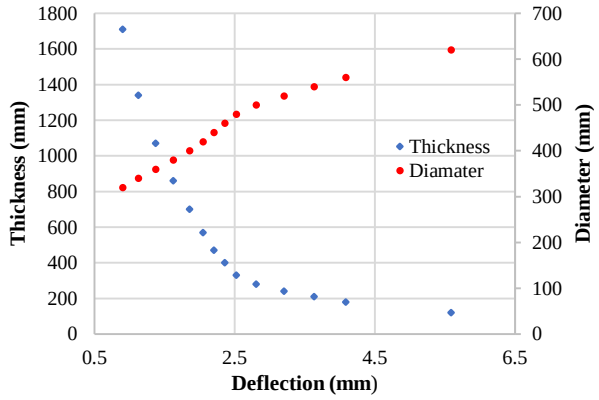

(a)

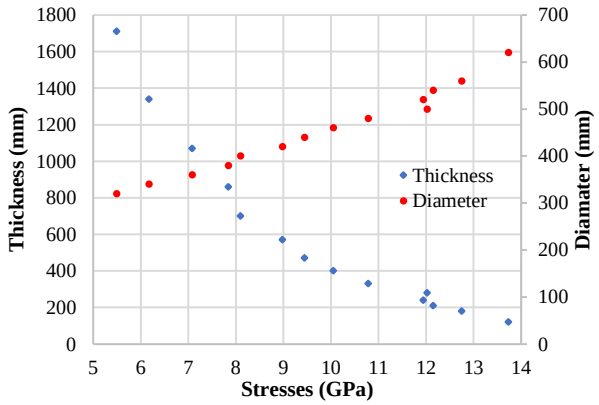

(b)

Figure 5 Plots for initial combinations; (a) stress (b) deflection

In the deflection plot as the diameter increases the deflection increases. Inversely, as thickness increases deflection decreases. The range of dimensions in which thickness and diameter are intersecting was used for optimization. The range of diameter used was 360 to 380 mm and the range of thickness was 860 to 1070 mm. FEA results were obtained by Abaqus, analysis was done to find the equivalent Von Mises stress and total deformation for different design combinations and static conditions. The resultant values are shown in Figure 6 (a) and 6 (b) for one of the cases of optimization 1.

In Figure 6 the red colour shows the maximum values while the blue shows the least. In Figure 6(a), red can be visualized at the hub which means maximum stress is being experienced there. The outer surface of the shaft experiences the least. In Figure 6(b), the maximum displacement is shown at the outer side of the shaft while the hub of the shaft shows the minimum displacement.

3.2. Optimization 2

For optimization, points from Fig. 5 were provided to the same MATLAB code and more precise combinations were obtained.

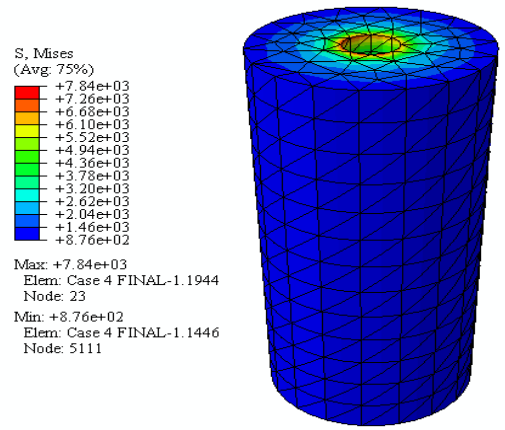

(a)

(b)

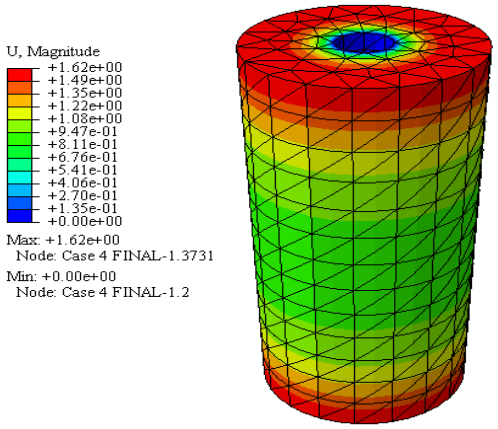

Figure 6 Plots for C4 (a) stress and (b) displacement

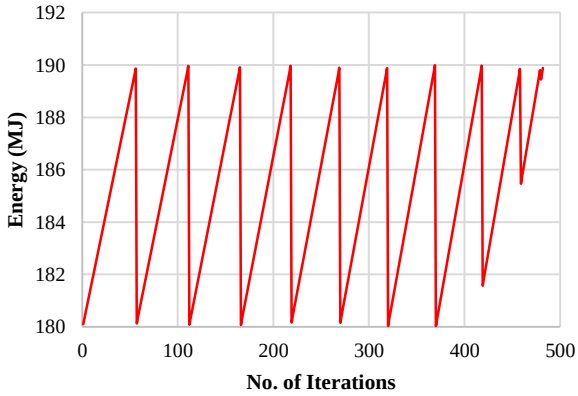

Figure 7 Second possible set of combinations of radius and thickness

The peak combinations from this graph are presented in Table 2. These combinations were then used for analysis, the results from the analysis are shown in Figure 8(a) and 8(b).

The results from Abaqus were used to collect the data presented in Table 2. Stresses and deflection were studied against diameter and thickness. In Figure 8(a) stresses show arbitrary trends against diameter and thickness.

Table 2 Thickness and Diameter Combinations for Optimization 1 and 2

Optimization 1					Optimization 2				
Configuration No.	**Diameter (mm)**	**Thickness (mm)**	**Stresses (GPa)**	**Deflection (mm)**	**Configuration No.**	**Diameter (mm)**	**Thickness (mm)**	**Stresses (GPa)**	**Deflection (mm)**
D1	360	1070	7.080	1.300	E1	376.0	899.0	7.581	1.490
D2	362	1047	6.631	1.320	E2	376.2	897.9	7.678	1.495
D3	364	1024	6.753	1.340	E3	376.4	895.9	7.633	1.498
D4	366	1002	6.859	1.370	E4	376.6	894.0	7.468	1.500
D5	368	980	6.919	1.390	E5	376.8	892.2	7.713	1.503
D6	370	959	7.058	1.420	E6	377.0	890.3	7.882	1.507
D7	372	939	7.207	1.450	E7	377.2	888.3	7.623	1.506
D8	374	919	7.138	1.470	E8	377.4	886.5	7.645	1.510
D9	376	899	7.581	1.490	E9	377.6	884.4	7.668	1.513
D10	378	880	7.700	1.520	E10	377.8	882.7	7.753	1.514
D11	380	862	7.783	1.540	E11	378.0	880.9	7.665	1.517

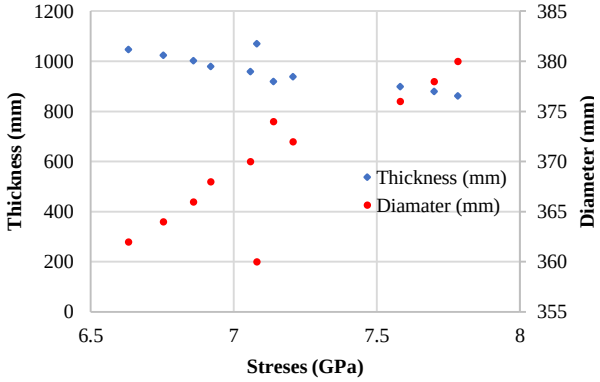

(a)

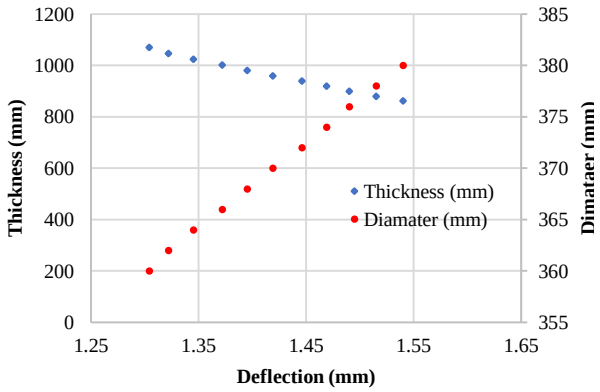

(b)

Figure 8 Plots for initial combinations; (a) stress (b) deflection

The deflection shows an almost linear trend in Figure 8(b). It is decreasing with increasing thickness and increases with increasing diameter. The range of dimensions between which the thickness and diameter are intersecting was used for optimization. The range of diameter used was 376 to 378 mm and the range of thickness was 880 to 899 mm.

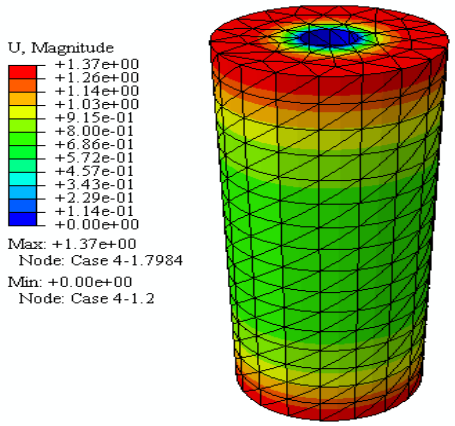

(a)

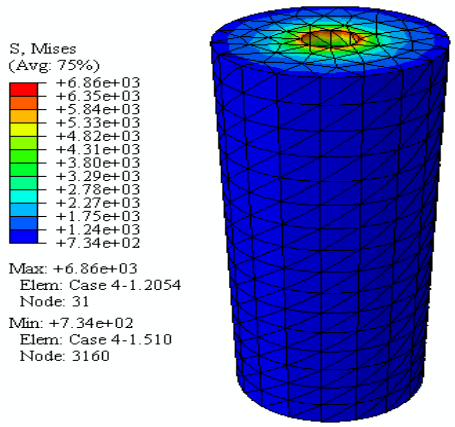

(b)

Figure 9 Plots for D4; (a) stress and (b) displacement

Figure 9(a) shows that maximum displacement is at the outer boundary of the shaft while the hub is

experiencing the minimum displacement. Figure 9(b) shows opposite trend, maximum stress is at the hub while the minimum stress is at the outer boundary.

3.3. Optimization 3

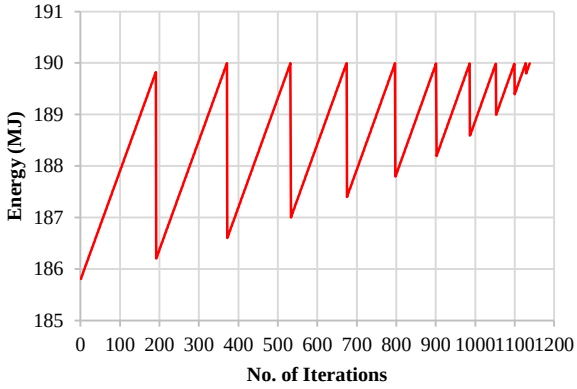

After the second optimization using the intersecting point of combination as limits, we again repeat the optimization procedure to get the most precise combination as shown in Figure 10.

Figure 10 Third optimized set of combinations

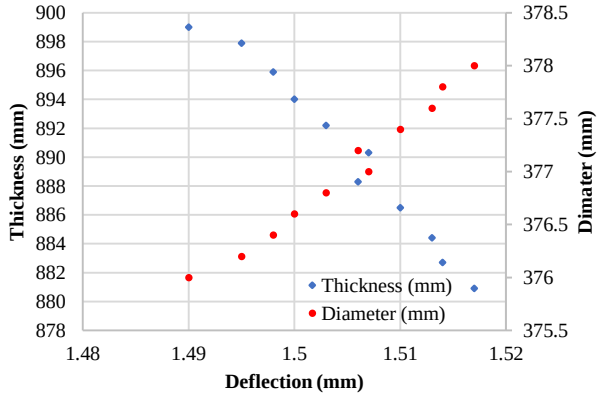

(a)

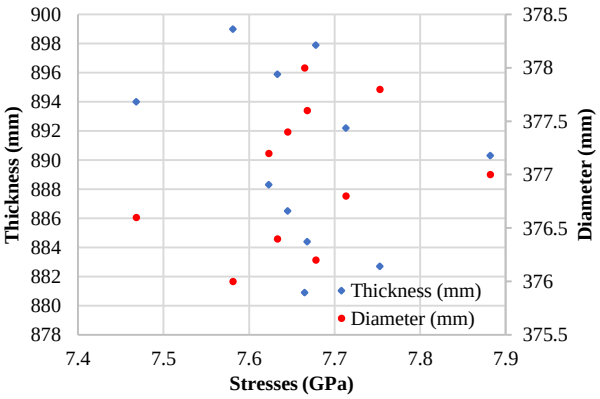

(b)

Figure 11 Plots for initial combinations; (a) stress (b) deflection

Table 2 shows the stresses and deflection results from Abaqus for optimization 3. In the stress plot, the arbitrary trend was shown between thickness and diameter as shown in Figure 11(a). The lines intersect at several points and it is not clear which pair of dimensions should be taken for further analysis. So, the deflection plot will be taken.

The deflection plot shows non-linear trend as shown in Figure 11(b). The thickness and diameter lines intersect at a point that represents two pairs of dimensions. Diameter is varying from 377 to 377.2 mm and thickness is varying from 888.3 to 890.3 mm. Average was taken to get the midpoint of the intersection of these dimensions. Diameter of the flywheel was 377.1 mm and its thickness was 889.3 mm. The peak combinations from this graph are presented in Table 2. Analysis results for one combination of optimization 3 are shown in Figure 12(a) and 12(b).

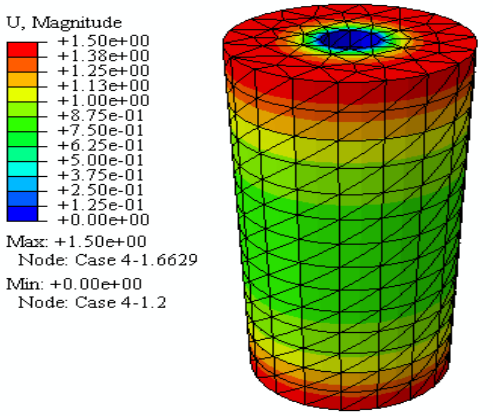

(a)

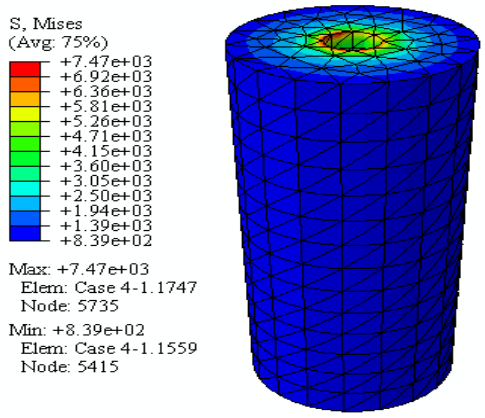

(a)

Figure 12 Plots for E4 (a) displacement and (b) stress

The colour coded scheme of Figure 6, Figure 9, and Figure 12 shows similar trends. Displacement is maximum at the outer surface while the minimum at the hub and, stress is maximum at the hub and minimum at the outer surface.

3.4. Final Shape Optimization

Table 3 Shape Optimization of flywheel

Case A **Varying Outer Thickness (±15%)**				**Case B** **Varying Inner Thickness (±15%)**			
Diameter Constant	**Thickness (mm)**	**Stresses (GPa)**	**Deflection (mm)**	**Diameter Constant**	**Thickness (mm)**	**Stresses (GPa)**	**Deflection (mm)**
	755.910	4.837	1.036		755.910	24.6	2.860
Inner	889.300	7.798	1.504	Outer	889.300	7.798	1.504
Thickness	1022.700	23.87	2.895	Thickness	1022.700	4.888	1.044
Constant				Constant			
Case C **Varying Side Surfaces (±15%)**				**Case D** **Varying Upper and Lower Surfaces (±15%)**			
Thickness Constant	**Diameter (mm)**	**Stresses (GPa)**	**Deflection (mm)**	**Diameter Constant**	**Thickness (mm)**	**Stresses (GPa)**	**Deflection (mm)**
	320.535	6.450	1.332		411.300	4.530	2.076
	377.100	7.798	1.504		444.650	7.798	1.504
	433.660	8.869	1.780		478	10.460	1.725

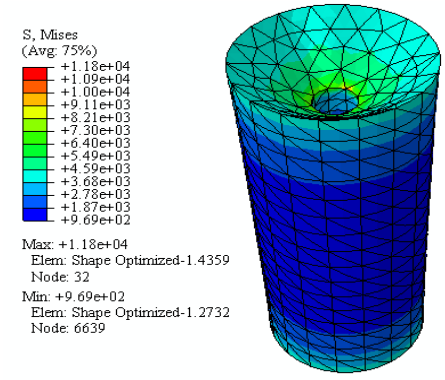

(a)

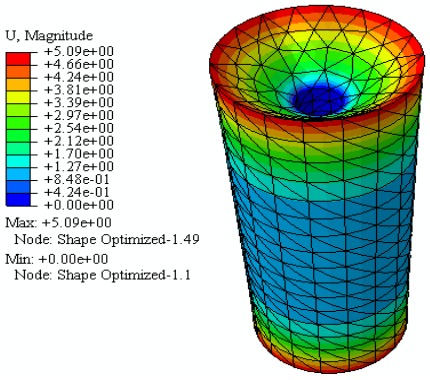

(b)

Figure 13 Plots for converged results (a) stress and (b) displacement

The model from each case with lowest values of stresses and deflection was selected and converged into a single model. The diameter and outer thickness of this model were 377.1 mm and 1022.7 mm respectively. The flywheel had a hub diameter of 90 mm and its inner thickness was 755.91 mm. The lower and upper cylindrical surfaces of the flywheel were converged inwards at 882.6 mm. This model was simulated in Abaqus, results showed that stress and deflection in flywheel was 11.8 GPa and 5.09 mm respectively. The results are presented in Table 3. The most feasible results were selected from four cases for FEA analysis and FEA results for that particular case are shown in Figure 13(a) and 13(b).

The converged results of Figure 13 show almost same trends as of initial optimization. But Figure 13(a) shows that stress is much minimal at the hub as compared to Figure 6(a), 9 (b), and 12(b). The displacement is showing safe values in the middle of the shaft while the corners of the shaft are not safe as shown in Figure 13(b). The models in Figure 6(b), 9(a) and 12(a) show intermediate values at the middle of the shaft while the corners show high values. The optimum design according to analytical data is converged flywheel rotor.

3. CONCLUSIONS

In this study, the shape optimization of the rotor Flywheel Energy Storage System (FESS) is presented. The initial dimensions of the rotor are determined from MATLAB and SolidWorks models are analysed on Abaqus. The dimensions are further optimized two times before selecting the most appropriate set of dimensions. The shape of the rotor is made complex and studied for stresses and deflection. The models giving least stresses and deflections are selected as the final design of rotor for Flywheel Energy Storage System.

The material used in this study was steel. When thickness of the rotor increases stresses decreases and deflection increases. Stresses and deflection were increased when diameter of the rotor increases. Initially, stress varies from 5.49 to 13.73 GPa and deflection varies

from 0.903 to 5.589 mm. In the first optimization, stress (deflection) varies from 6.6 to 7.783 GPa (1.304 to 1.54 mm). In the second optimization, stress (deflection) variation was 7.468 to 7.882 GPa (1.49 to 1.517 mm). The final model has stress and deflection of 11.8 GPa and 5.09 mm respectively. The approach used in this study was general static analysis in which aerodynamics, friction and vibrations were ignored. A better approach using dynamic analysis (rotor balancing and aerodynamic system) can be used in future studies. The material used in this study was basic material (steel), modern composite materials can be used in future studies to obtain better results.

AUTHORS' CONTRIBUTIONS

Kainat Riaz: Original Draft Writing, Formal Analysis.

Syeda Fatima Imam: Original Draft Writing, Formal Analysis.

Nida Ilyas: Original Draft Writing, Formal Analysis.

Zia ul Rehman Tahir: Conceptualization, Methodology, Investigation, Validation.

Muhammad Taimoor Adil: Methodology, Investigation, Validation, Writing.

Sajeer Ahmad: Writing, Review/Editing.

Muhammad Abdullah: Writing, Review/Editing.

Tariq Ali: Writing, Review/Editing, Formatting,

Imran Amin: Review/Editing, Formatting.

Ahmad Hassan: Review/Editing,

Najum ud Din: Review/Editing.

Muhammad Saad: Review/Editing.

ACKNOWLEDGMENTS

The authors would like to acknowledge Department of Mechanical Engineering, University of Engineering and Technology, Lahore for providing computer facilities used for this study.

REFERENCES

[1] Genta, G., *Kinetic energy storage: theory and practice of advanced flywheel systems*. 2014: Butterworth-Heinemann.

[2] Parfomak, P.W., *Energy storage for power grids and electric transportation: a technology assessment*. 2012, Congressional Research Service Washington, DC, USA.

[3] Akhil, A.A., et al., *DOE/EPRI 2013 electricity storage handbook in collaboration with NRECA*. Vol. 1. 2013: Sandia National Laboratories Albuquerque, NM, USA.

[4] Okou, R., et al., *The potential impact of small-scale flywheel energy storage technology on Uganda's energy sector %J Journal of Energy in Southern Africa*. 2009. **20**: p. 14-19.

[5] Chen, H., et al., *Progress in electrical energy storage system: A critical review*. Progress in Natural Science, 2009. **19**(3): p. 291-312.

[6] Medina, P., et al. *Electrical Energy Storage Systems: Technologies' State-of-the-Art, Techno-economic Benefits and Applications Analysis*. in *2014 47th Hawaii International Conference on System Sciences*. 2014.

[7] Hadjipaschalis, I., A. Poullikkas, and V. Efthimiou, *Overview of current and future energy storage technologies for electric power applications.* Renewable and Sustainable Energy Reviews, 2009. **13**(6): p. 1513-1522.

[8] Hebner, R., J. Beno, and A. Walls, *Flywheel batteries come around again.* IEEE Spectrum, 2002. **39**(4): p. 46-51.

[9] Bolund, B., H. Bernhoff, and M. Leijon, *Flywheel energy and power storage systems.* Renewable and Sustainable Energy Reviews, 2007. **11**(2): p. 235-258.

[10] Tang, C.-L., et al., *Rotor dynamics analysis and experiment study of the flywheel spin test system.* Journal of Mechanical Science and Technology, 2012. **26**(9): p. 2669-2677.

[11] Adams, M.L., *Rotating machinery vibration: from analysis to troubleshooting*. 2000: CRC Press.

[12] Arnold, S.M., A.F. Saleeb, and N.R. Al-Zoubi, *Deformation and life analysis of composite flywheel disk systems.* Composites Part B: Engineering, 2002. **33**(6): p. 433-459.

[13] Babuska, V., et al. *A review of technology developments in flywheel attitude control and energy transmission systems*. in *2004 IEEE Aerospace Conference Proceedings (IEEE Cat. No.04TH8720)*. 2004.

[14] Liu, H. and J. Jiang, *Flywheel energy storage—An upswing technology for energy sustainability*. Energy and Buildings, 2007. **39**(5): p. 599-604.

[15] Vance, J.M., F.Y. Zeidan, and B.G. Murphy, *Machinery vibration and rotordynamics*. 2010: John Wiley & Sons.

[16] Krack, M., M. Secanel, and P.J.J.O.A.M. Mertiny, *Advanced optimization strategies for cost-sensitive design of energy storage flywheel rotors.* 2011. **43**(2): p. 65-78.

[17] Ha, S.K., et al., *Design and Spin Test of a Hybrid Composite Flywheel Rotor with a Split Type Hub*. Journal of Composite Materials, 2006. **40**(23): p. 2113-2130.

[18] Dell, R.M. and D.A.J. Rand, *Energy storage — a key technology for global energy sustainability*. Journal of Power Sources, 2001. **100**(1): p. 2-17.

[19] Wagner, R.C., D.R. Boyle, and K. Decker. *Commercialization of flywheel energy storage technology on the international space station*. in *IECEC '02. 2002 37th Intersociety Energy Conversion Engineering Conference, 2002.* 2002.

[20] Yimin, G., et al. *Flywheel electric motor/generator characterization for hybrid vehicles*. in *2003 IEEE 58th Vehicular Technology Conference. VTC 2003-Fall (IEEE Cat. No.03CH37484)*. 2003.

[21] Shimoyama, H., et al., *Study on hybrid vehicle using constant pressure hydraulic system with flywheel for energy storage*. 2004, SAE Technical Paper.

[22] Kohari, Z. and I. Vajda, *Losses of flywheel energy storages and joint operation with solar cells.* Journal of Materials Processing Technology, 2005. **161**(1): p. 62-65.

[23] Owusu-Ansah, P., H. Yefa, and A. Misbawu. *Rotor Dynamic Modeling and Analysis of a Flywheel Rotor*. in *Proceedings of the 2015 International Conference on Electronic Science and Automation Control*. 2015. Atlantis Press.

[24] Hodžić, E., et al., *NUMERICAL ANALYSIS OF THE ROTOR OF A HIGH-SPEED INTEGRATED FLYWHEEL ENERGY STORAGE SYSTEM.*

[25] Arani, A.A.K., et al., *Review of Flywheel Energy Storage Systems structures and applications in power systems and microgrids.* Renewable and Sustainable Energy Reviews, 2017. **69**: p. 9-18.

[26] Kale, V. and M. Secanell, *A comparative study between optimal metal and composite rotors for flywheel energy storage systems.* Energy Reports, 2018. **4**: p. 576-585.

[27] Kress, G.R., *Shape optimization of a flywheel.* Structural and Multidisciplinary Optimization, 2000. **19**(1): p. 74-81.

[28] Chan, C.C., *The state of the art of electric and hybrid vehicles.* Proceedings of the IEEE, 2002. **90**(2): p. 247-275.

[29] Mitchell, L., *A commentary on'The energy review'.* Power Engineering Journal, 2002. **16**(4): p. 175-181.

[30] Hou, Y., et al., *Size effect on mechanical properties and deformation behavior of pure copper wires considering free surface grains.* Materials, 2020. **13**(20): p. 4563.